IMEKO 24th TC3, 14th TC5, 6th TC16 and 5th TC22 International Conference
11 – 13 October 2022, Cavtat-Dubrovnik, Croatia

EXPERIMENTAL RESULTS OF MEASUREMENT HINGE FLEXURE STIFFNESS DETERMINATION

K. Geva[1], H. Kahmann[2], C. Schlegel[3], R. Kumme[4]

Physikalisch-Technische Bundesanstalt, Braunschweig, Germany
[1] kai.geva@ptb.de, [2] holger.kahmann@ptb.de, [3] christian.schlegel@ptb.de, [4] rolf.kumme@ptb.de

Abstract:

A hinge measurement flexure calibration set-up for stiffness measurements has been built at the Physikalisch-Technische Bundesanstalt (PTB) to estimate parasitic loads on PTB's 5 MN·m torque standard machine (TSM). This paper describes the improvements made to a measurement flexure calibration set-up made since its first presentation. The list of measurement uncertainty influences is refined. Initial results of a combined transversal force and bending and torque moment stiffness measurement are presented and compared to a previous finite element analysis.

Keywords: stiffness measurement; multi-axis measurement; hinge flexure; torque standard machine

1. INTRODUCTION

The increasing number of wind turbines has prompted manufacturers to economically optimise such turbines. A wind turbine's efficiency is determined by applying a wind simulating torque onto a nacelle in a test bench and measuring the electrical power output and the mechanical power input (i.e., the torque and the rotational speed). In Germany, modern wind turbines generate electric power (on average) of up to 4 MW onshore and up to 5 MW offshore, which correlates to an approximate input torque of 4 MN·m to 5 MN·m [1]. Test-bench measurement systems presently lack the ability to validate the torque moment applied in a test, thus creating uncertainty in terms of the efficiency determined [2].

At PTB, a new 5 MN·m torque standard machine, as depicted in Figure 1, is being constructed to calibrate torque transducers up to 5 MN·m [3]. The torque standard machine comprises an actuator side and a measurement side (in Figure 1 on the right and left, respectively). The actuator side consists of eight hydraulic cylinders which apply force onto the actuator lever. Two primary vertical cylinders generate a torque around a horizontal axis; additional cylinders can superpose axial forces and bending moments. The combined load is introduced to the device under calibration and transferred to the measurement side.

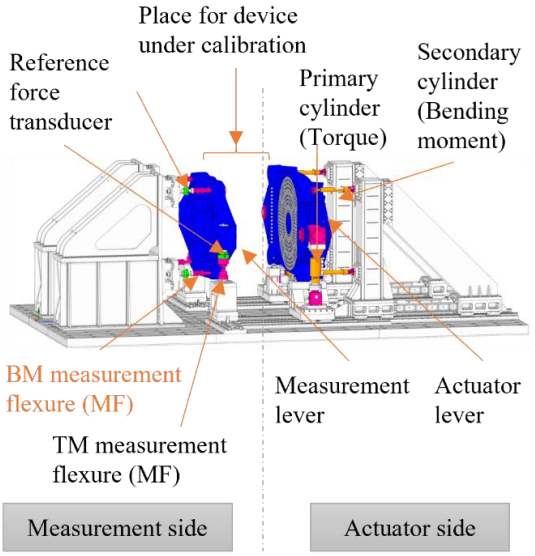

Figure 1: 5 MN·m torque standard machine

The measurement lever is connected to the flexure hinges. There exist two vertical hinge flexures and four horizontal flexures. The vertical group is called the torque moment hinge flexure and the horizontal group is called the bending moment hinge flexure. The two vertical force transducers measure the main lever arm force and allow to determine the generated torque.

The hinge flexures provide a frictionless bearing for the measurement lever. Even though force and moment shunts to the calibration torque are inevitable, the unique reproduction enables the reproducible measurement of these shunts to compensate the systematic deviation. This paper focusses only on BM measurement flexures (marked orange in Figure 1).

A common transducer based on strain gauge technology is not recommended when high axial force meets transversal force because of crosstalk. A suggested method for overcoming these difficulties utilises the elastic feature of the hinge flexure and are defined as measurement flexures (MFs) hereafter. The measurement flexures' top flange displacement can be tracked indirectly during TSM calibration with an interferometer. The

interferometer measures the tangential displacement of the lever and thus the rotational angle of the lever. Knowing the position of the measurement flexure relative to the pivot point reveals its tangential displacement. If the stiffness under the active load combination is known, the force and moment shunts of each measurement flexure can be measured. The tangential force and the torque moment contribute to the systematic deviation of the overall torque measurement M_z. The set-up design was presented in [4] and an initial measurement budget for load application was introduced.

This paper presents the determination of the bending moment measurement flexures. A few modifications to the calibration set-up presented are necessary to reduce and validate the measurement uncertainty. Finally, the FE results are compared with the experimental results.

2. METHOD

2.1. Measurement Flexure Calibration Set-up

The calibration set-up is depicted in

Figure 2 for the bending moment (BM) load scenario and in Figure 3 for the torque moment (TM) load scenario. For the calibration set-up, the MF under test is mounted vertically to the T-slot plate field. On top of the MF, the lever for the respective load scenario is attached. The force is applied via a thin metal foil at the end of the lever arm and provided via calibrated mass disks. Because the force must be aligned horizontally to the MF, the gravitational force is redirected by a pulley supported by a frame on the right side.

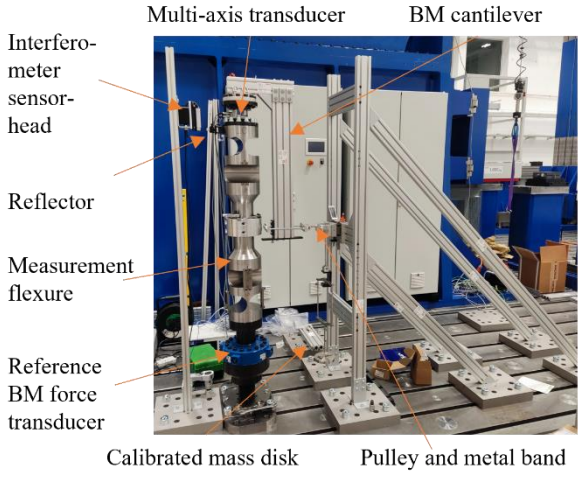

Figure 2: Calibration set-up for BM load scenario

The bending moment load scenario lever consists of a cantilever with a short horizontal part and a vertical part extending to the middle of an MF. The bending moment load scenario imitates the tangential force the MF receives from the lever. Because the much stiffer lever displacement forces the MF connection flange to follow, a bending moment is generated which is zero in the middle of the MF. The interferometer reflector is placed near the MF top flange at the shaft.

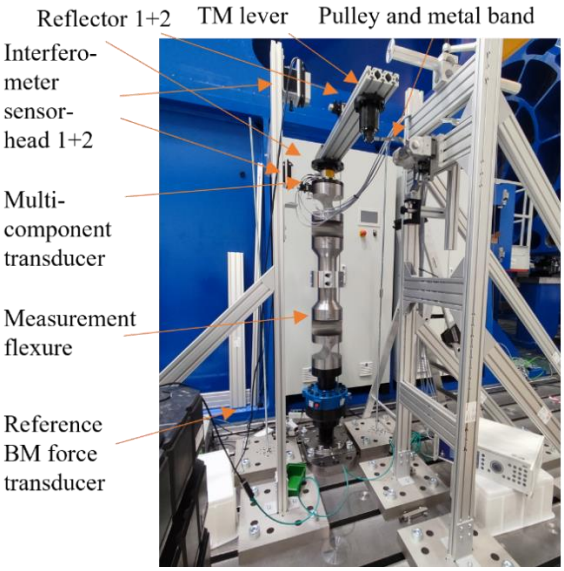

Figure 3: Calibration set-up for TM load scenario

The torque moment load scenario has a straight lever to whose end the metal band is attached. To compensate the rotation caused by the torque, the force introduction point is supported by an axial contact ball bearing to keep the force aligned with the MF orientation and to reduce transversal forces.

Several changes have been made to the original design presented in [4]. It was necessary to change the bearing supporting the pulley for the force redirection to reduce the friction.

Furthermore, a multi-axis transducer between the MF and the lever was integrated. allowing the expected load values in [4] to be validated.

Another adjustment was necessary because the FE analysis of the torque load scenario in [5] implied there was a major difference in the torque stiffness determination when an axial force was applied onto the MF while also applying torque. Therefore, an additional traverse was designed to apply an axial force.

2.2. Measurement Uncertainty Budget Refinement for Force and Torque

The modification mentioned in the section above and a few restrictions during the measurement series necessitated a refinement of the measurement uncertainty budget (MUB) presented in [5].

The friction due to the bushing exchange decreases to 0.11 N at the maximum load step, reducing the measurement uncertainty. As the rolling resistance coefficient is presented as 0.001 to 0.002 in the technical specification sheet, a measurement uncertainty of 0.081 N must be considered here. The horizontal angle deviation γ between the force introduced to the lever and the pulley for force redirection becomes negligible.

The tilt angle of the MF top flange to the plate field ε and the resulting angle δ from the vertical misalignment of the force and the pulley are higher than expected in the former MUB. Reducing the rotation alignment around the MF *z*-axis φ to zero (as expected in the theoretical analysis) was not possible. All the resulting misalignment angles were measured via a laser tracker. The average angles were calculated, their respective maximum deviations were determined, and a rectangular uncertainty distribution was assumed. Their contribution to the load application is shown in Table 1 and Table 2.

This yielded the following new model equation for force:

$$F_{\mathrm{BM,i}} = m_{\mathrm{i}} \cdot g_{\mathrm{loc}} \cdot \left(1 - \frac{\rho_{\mathrm{L}}}{\rho_{\mathrm{m}}}\right) \cdot \cos(\varphi\,) \cdot \cos(\delta)\cos(\varepsilon) + \Delta F_{\mathrm{PM}} - \Delta F_{\mathrm{R}} \quad (1)$$

where ρ_{L} is the ambient air density, ρ_{m} is the density of the mass disks, ΔF_{PM} is the deviation due to pendulum motion of the mass disks and ΔF_{R} is the friction caused by the bearing.

The new force MUB at load step 120 N is shown in Table 1. The last column named "Ind." is specified as relative measurement uncertainty index. It is evident that the highest MU contribution is due to poor MF rotation alignment around its *z*-axis.

Table 1: Measurement uncertainty budget of force calibration set-up at nominal load step 120 N

Quantity	Value	MU (k = 2)	Unit	Ind. / %
ε	0.001 4	0.04	rad	0.1
δ	0.003 4	0.001 2	rad	1.1
φ	0.035	0.011	rad	98.1
ρ_{M}	7 927	23.7	kg·m^{-3}	0.5
ΔF_{PM}	0	0.1	N	0.1
∑Rest	-	-	-	< 0.1

A revision of the MUB for the torque moment was also necessary (Table 2) and yielded the following new model equation for torque:

$$M_{\mathrm{TM,i}} = F_{\mathrm{TM,i}} \cdot l_{\mathrm{TM}} \cdot \cos(\delta) \cdot \cos(\varepsilon) \quad (2)$$

The MU for transversal force decreased significantly due to friction reduction, making the tilt of the MF top flange to the gravitation direction and the lever arm length measurement more significant.

Table 2: Measurement uncertainty budget of force calibration set-up at nominal load step 94 N·m

Quantity	Value	MU (k = 2)	Unit	Ind. / %
$F_{\mathrm{TM,120}}$	115.81	1.1	N	0.0
l_{TM}	0.72	0.000 11	m	18.7
δ	0	0.004 65	rad	3.0
ε	0	0.001 86	rad	78.3

2.3. Measurement Uncertainty Budget of Multi-axis Transducer

To validate the model equation and its measurement uncertainty analysis, a multi-axis transducer is used. Below, a short analysis of the transducer measurement uncertainty is presented. The transducer has been calibrated and provides information for crosstalk correction. The measurement uncertainty budget is presented in Table 3. The model equation is as follows:

$$F_y = F_{y,\mathrm{meas}} \cdot \cos\alpha \cdot k_{\mathrm{Lin}} \cdot k_{\mathrm{Hyst}} \cdot k_{\mathrm{Reprod}} + k_{\mathrm{T}} \cdot \Delta T + \Delta F_0 + \Delta F_{\mathrm{Ind}} + \Delta F_{\mathrm{Drift}} \quad (3)$$

Table 3: Measurement uncertainty budget for F_y measuring channel of MKA transducer at 120 N

Quantity	Value	MU (k = 2)	Unit	Ind. / %
$\boldsymbol{F_{y,\mathrm{meas}}}$	116.3	0.59	N	11.0
$\boldsymbol{\alpha}$	0.0	0.000 529	°	0.1
$\boldsymbol{k_{\mathrm{Lin}}}$	1.0	0.002	-	1.7
$\boldsymbol{k_{\mathrm{Hyst}}}$	1.0	0.001	-	0.4
$\boldsymbol{k_{\mathrm{T}}}$	0	0.000 04	N·K^{-1}	0.0
$\boldsymbol{\Delta T}$	0	0.538	K	0.0
$\boldsymbol{\Delta F_0}$	0	1.66	N	86.7
∑Rest	-	-	-	0.0

The coefficient uncertainties for linearity k_{Lin}, hysteresis k_{Hyst} and reproducibility k_{Reprod} are taken from the data sheet of the MKA I GTM transducer model. The angle α represents the misalignment between the transducer and the MF. The temperature coefficient set is the same as the temperature coefficient for 0 °C in the data sheet. It was necessary to include ΔF_0 as the set-up did not allow the zero values of each series of measurements to be measured easily. Zero values were logged at the beginning of the set-up of each MF. For all other set-ups, the average value of all zero values was calculated and the maximum deviation taken into account as a standard uncertainty. In the MUB, it is evident that the zero deviation has a great influence.

The measurement uncertainty budget is presented in Table 4. The model (equation (4)) is analogous to equation (3)

$$M_z = M_{z,\mathrm{meas}} \cdot \cos\alpha \cdot k_{\mathrm{Lin}} \cdot k_{\mathrm{Hyst}} \cdot k_{\mathrm{Reprod}} + k_{\mathrm{T}} \cdot \Delta T + \Delta M_0 + \Delta M_{\mathrm{Ind}} + \Delta M_{\mathrm{Drift}} \quad (4)$$

Table 4: Measurement uncertainty budget for M_z measuring channel of the MKA transducer at 83 N·m

Quantity	Value	MU (k = 2)	Unit	Ind. / %
$M_{z,\mathrm{meas}}$	83.4	0.44	N·m	83.8
α	0.0	0.000 529	°	0.8
k_{Lin}	1.0	0.002	-	11.9
k_{Hyst}	1.0	0.001	-	3.0
k_{Reprod}	1.0	0.000 001	-	0.0
k_{T}	0	0.000 04	N·m K^{-1}	0.0
ΔT	0	0.538	K	0.0
ΔM_0	0	0.03	N·m	0.1
ΔM_{Ind}	0	0.01	N·m	0.0
$\Delta M_{\mathrm{Drift}}$	0	0.001 4	N·m	0.0

The absolute measurement uncertainties gathered from the model equation of the MKA transducer and the load and torque application in the calibration set-up are depicted in Figure 4. The force applied in the calibration set-up has an uncertainty < 3 N and the torque uncertainty is < 1.5 N·m. The absolute measurement uncertainty for the force measurement of the MKA transducer in this specific application is < 4 N and for torque measurement < 2 N·m. The uncertainties of the force and torque measurements of the transducer are higher than the theoretical uncertainties gained from both model equations but are small enough to validate the theoretical analysis.

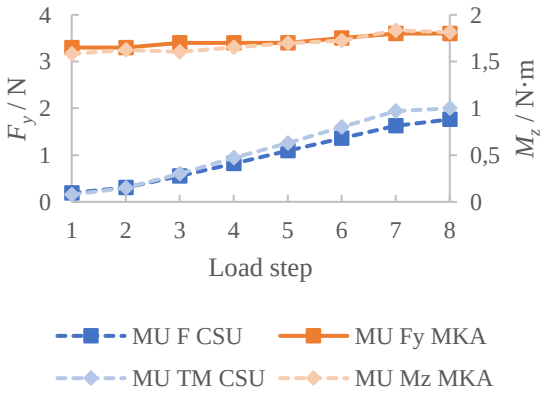

Figure 4: Measurement uncertainties for MKA transducer and load application of calibration set-up

During the measurement series, the transducers were replaced with another uncalibrated multi-axis transducer. Its measurement uncertainty is much higher than that of the MKA because the crosstalk influence was not compensated since both transducers were built in a similar way. The measurement values indicated whether only the main sensitivities of the uncalibrated transducer were taken into account and whether the main sensitivities were extended by crosstalk sensitivities from the MKA. The average difference was 22 % greater. Applying the 50 % method yielded a half width of 11 % for a rectangle. Even though most of the series had to be performed with the uncalibrated transducer, important information regarding the sensitivity of the MF were revealed. The stiffness factors shown below are only temporary until the transducers have been calibrated.

2.4. Stiffness Determination

Before the lever was attached to the MF, the measurement signal was adjusted to zero. If a zero adjustment was not possible, the average zero value was assumed. Then, the mass disks were placed manually onto the hanger, pulling the lever. In the evaluation, for each load step 100 s before and after (if available) were taken into account to obtain an average value for each force or torque and each displacement at one load step. By determining the increase of the linear regression with an offset of zero, the BM stiffness was calculated as follows:

$$k_{\mathrm{Stiff,BM}} = \frac{\sum_{i=1}^{n}(u_{\mathrm{i}} - \bar{u}) \cdot \left(F_{\mathrm{T,i}} - \bar{F}_T\right)}{\sum_{i=1}^{n}(u_{\mathrm{i}} - \bar{u})^2} \quad (5)$$

with n being the number of all load steps and i the load step.

For TM stiffness, it was necessary to measure a rotation via the displacement of two retro reflectors. If the radius of the measurement flexure was known, the first reflector's position was the same as in the BM load case. The second reflector was mounted to the lever because it was not possible to mount the reflector to the shaft. This led to a rotation "shunt" of the transducer and the bending of the of lever. This influence was investigated subsequently in FE. The torsion of the transducer and other adapters and the bending of the lever were subtracted to obtain the pure rotation of the measurement flexure. The displacement in the FE analysis was validated via the measurement displacements in section 3.3. After the rotation correction, the stiffness coefficient was determined analogously to the bending moment load scenario as follows:

$$k_{\mathrm{Stiff,TM}} = \frac{\sum_{i=1}^{n}(\gamma_{\mathrm{i}} - \bar{\gamma}) \cdot \left(M_{\mathrm{T,i}} - \bar{M}_{\mathrm{T}}\right)}{\sum_{i=1}^{n}(\gamma_{\mathrm{i}} - \bar{\gamma})^2} \quad (6)$$

with γ being the torsional angle.

3. RESULTS

3.1. Measurement Uncertainty Budget Validation of Calibration Set-up

Figure 5 depicts the load steps as calculated in the model equation and the average measured load steps measured via MKA and LVS. There is an intersection of the range covered by the upper and lower limit of the expected values and the band covered by the MU of the MKA. The LVS measurements are added for reasons of complementarity.

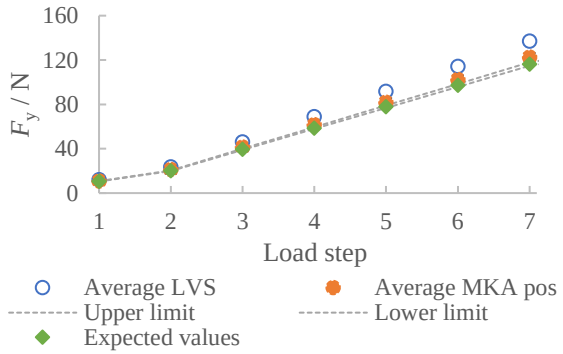

Figure 5: Validation of bending moment load steps

The difference in the LVS values is much greater than with the MKA; however, considering the high MU of 11 %, the expected values are still within the uncertainty range.

Figure 6 depicts the load steps for the torque moment. Although the torque moment is measured only via the LVS replacement transducer, the values measured by the transducer match the expected values very well. In summary, the comparison of expected values of the model equations presented above shows good consistency and may be used for stiffness determination.

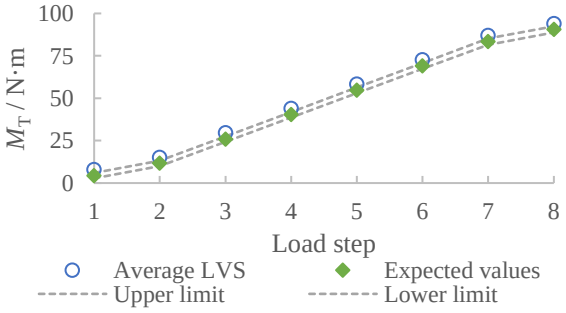

Figure 6: Validation of torque moment load steps

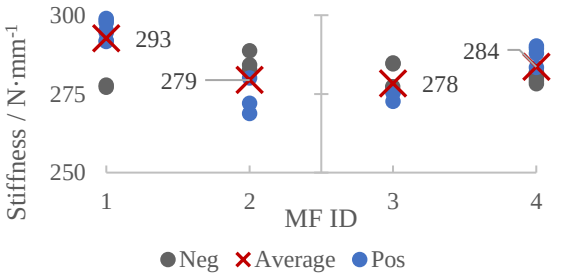

Figure 7: BM stiffness coefficient

3.2. BM Stiffness Evaluation

The BM stiffness coefficients are shown in Figure 7. To categorize the stiffness, each MF is labelled with an ID from 1 to 4. ID 1 and ID 2 are the MF at the top with a wider shaft and ID 3 and ID 4 are at the bottom. Evaluation here is more difficult because ID 2 is measured only via the MKA transducer and ID 1, ID 3 and ID 4 are measured via the LVS transducer. As can be seen in Figure 5 and Figure 6, the indication of the uncalibrated LVS is higher than that of the calibrated MKA. This indicates that the BM stiffness measured via LVS may be smaller.

The BM stiffness of both top MFs ID 1 and ID 2 deviate from each other by 4.3 %. The deviation is higher than between ID 3 and ID 4, which is 1.9 %. One reason for the higher deviation is the use of two different transducers for ID 1 and ID 2. Although the LVS transducer has a very large measurement uncertainty, it is possible to achieve a good reproducibility with both bottom MFs. In [5], an FE was performed to determine the deformation and the load created by the calibration set-up. The BM stiffness was found to be 324 N·mm^{-1}.

The BM stiffness coefficient of MF ID 2 measured via MKA deviates from the FE analysis in [5] by about 16 %. The significant deviation strongly reinforces the idea that an experimental stiffness coefficient determination is necessary. The average BM stiffness coefficient of ID 2 measured via MKA is 279 N·mm^{-1} and the average value for ID 1, ID 2 and ID 3 is 284 N·mm^{-1}.

3.3. TM Stiffness Evaluation

The FE analysis [5] determined the torque stiffness to be 3.81×10^5 N·m·rad^{-1} for the top MF. One problem with the previous evaluation method is that the average rotation value from all top surface nodes was calculated. This average rotation value did not match the results by a factor of ten if the rotation was calculated via two single displacement measurements and a known radius. Adapting the evaluation in such a way that the interferometer measured the displacement allowed the FE to reproduce the measurement well enough (see Figure 8). The gradient deviation from the rotation measurement is 14.06 %.

During the measurement series, the issue of where to place the second reflector arose. To measure the rotation of the MF, the reflector would have to be mounted to the outer shaft surface adjacent to the top MF flange. It was not possible to mount the reflector in such a way that the laser reflection would be in line with the displacement direction. The reflector position was therefore shifted to the TM lever. The problem with measuring the rotation in this way is that it is the sum of the rotation of the MF, the transducer, the

lever and all adapter parts. Because the sum of all rotations is linear, it is possible to calculate a fixed factor that allows the rotation of the MF to be calculated by multiplying the factor by the sum of all rotations. The FE analysis finds a factor of the stiffness from the rotation sum and the MF of 5.9.

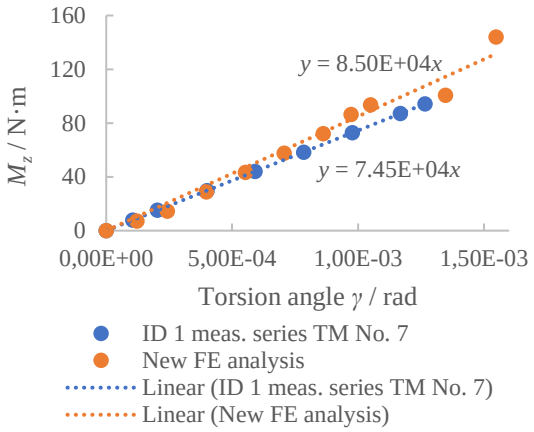

Figure 8: Revised FE analysis compared to rotation measurement with two single displacements

The corrected TM stiffness coefficients are depicted in Figure 9. Except for two outliers at ID 4, all measurements are reproducible. The average TM stiffness coefficient of the top MF TM stiffness is 1.28×10^4 N·m·rad^{-1}; for the lowest stiffness, it is 1.20×10^4 N·m·rad^{-1}.

The torque stiffness must be corrected via the torsion stiffness of the transducers. The previous FE analysis in [5] indicated that the addition of axial force would change the torque stiffness. The experimental results in Figure 9 did not reproduce the effect of the axial force.

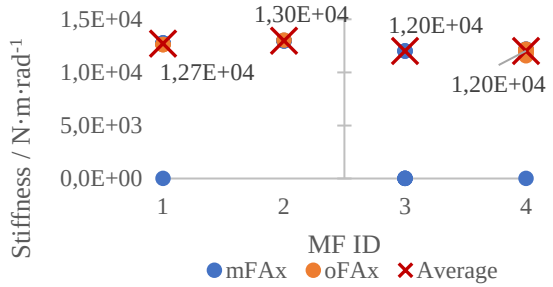

Figure 9: TM stiffness coefficient

4. CONCLUSIONS

Obtaining more precise stiffness measurement results for both BM and TM stiffness requires a multi-axis calibration of the LVS and allows further investigations on the MF measurement characterisation. Recalibration of the MF requires certain optimisations to the calibration set-up. For example, the torque stiffness was be refined by adding a mounting option directly at the shaft. A way must be found to measure the zero value of the transducer before a measurement series starts. The next optimisation to take place should be the rotation alignment of the MF. The results for BM and TM stiffness measurements can be considered for the global torque measurement in the TSM. The MU must be determined in the next step to reduce the overall uncertainty of the global M_z. This can only be done if the MU is calibrated after the LVS.

5. SUMMARY

Modifications to the calibration set-up already presented in [5] are described. The impact on the MUB force and torque are presented. Newly integrated transducers of theoretical force and torque values are validated. Results for force and torque stiffness are shown.

6. REFERENCES

[1] Deutsche WindGuard, “Status of Offshore Wind Energy Development in Germany”, 2021. Online [Accessed 20220930]: https://www.windguard.com/publications-wind-energy-statistics.html

[2] C. Schlegel, H. Kahmann, R. Kumme, “MN·m torque calibration for nacelle test benches using transfer standards”, Acta IMEKO, vol. 5, no. 4, 2016, pp. 12-18. DOI: 10.21014/acta_imeko.v5i4.414

[3] H. Kahmann, C. Schlegel, R. Kumme, D. Röske, “Principle and Design of a 5 MN·m Torque Standard Machine”, Proc. of 23rd IMEKO TC3 Conference, Helsinki, Finland, 30 May - 01 June 2017. Online [Accessed 20221221]: https://www.imeko.org/publications/tc3-2017/IMEKO-TC3-2017-037.pdf

[4] K. Geva, H. Kahmann, C. Schlegel, R. Kumme, “Analysis of the measurement uncertainty of a new measurement flexure calibration set-up”, Acta IMEKO, vol. 9, no. 5, 2020, pp. 173-178. DOI: 10.21014/acta_imeko.v9i5.963

[5] K. Geva, H. Kahmann, C. Schlegel, R. Kumme, “Measurement uncertainty analysis of a measurement flexure hinge in a torque standard machine”, J. Sens. Sens. Syst., vol. 11, 2022, pp. 201-209. DOI: 10.5194/jsss-11-201-2022